

# Searching for stellar cycles on low mass stars using *TESS* data

Gavin Ramsay<sup>1</sup>, Pasi Hakala<sup>2</sup>, J. Gerry Doyle<sup>1</sup>

<sup>1</sup> Armagh Observatory and Planetarium, College Hill, Armagh, BT61 9DG, N. Ireland, UK

<sup>2</sup> Finnish Centre for Astronomy with ESO (FINCA), Quantum, Vesilinnantie 5, FI-20014, University of Turku, Finland  
e-mail: gavin.ramsay@armagh.ac.uk

Accepted 9 July 2024

## ABSTRACT

We have searched for stellar activity cycles in late low mass M dwarfs (M0–M6) located in the *TESS* north and south continuous viewing zones using data from sectors 1–61 (Cycle 1 to part way through Cycle 5). We utilise *TESS*-SPOC data which initially had a cadence of 30 min but reducing to 10 min in Cycles 3. In addition, we require each star to be observed in at least 6 sectors in each North/South Cycle: 1,950 low mass stars meet these criteria. Strong evidence was seen in 245 stars for a very stable photometric variation which we assume to be a signature of the stars rotation period. We did a similar study for Solar-like stars and found that 194 out of 1432 stars had a very stable modulation. We then searched for evidence of a variation in the rotational amplitude. We found 26 low mass stars showed evidence of variability in their photometric amplitude and only one Solar-like star. Some show a monotonic trend over 3–4 yrs whilst other show shorter term variations. We determine the predicted cycle durations of these stars using the relationship found by Irving et al. (2023) using an estimate of the stars Rossby number. Finally we find a marginally statistically significant correlation between the range in the rotational amplitude modulation and the rotation period.

**Key words.** Physical data and processes: magnetic fields – Stars: activity, flares, low-mass, late-type, rotation

## 1. Introduction

Low mass stars account for nearly 3/4 of the stars in our local neighbourhood (Henry et al. 2006). In spite of this, it is only in the last few decades that a more intense focus has returned to these low luminosity stars. Within the MV spectral type, stars have masses in the range 0.08–0.6  $M_{\odot}$  (M9V–M0V), becoming fully convective around early-to mid M. The reason for the renewed interest in these stars is due to exoplanets producing a greater transit depth in these small stars making them easier to detect. Furthermore, many of these stars are active, especially fully convective stars (e.g. Pettersen (1989)), which provides insight into how fully convective stars generate and sustain a global magnetic field, which is of interest to the field of magnetism in general.

Moreover, the instruments to study stars of all kinds has radically changed since the first exoplanets were detected. Prior to the launch of *Corot* and *Kepler*, several groups attempted ground-based multi-telescope observations of single stars (e.g. Rodono et al. (1986); Doyle et al. (1988a,b, 1993)). What these series of space missions facilitated (amongst many other things) was the measurement of the rotation period for a large number of stars (McQuillan et al. 2014) and a comprehensive search for flares from stars with a wide range of spectral type (Davenport 2016). In turn, this allows for the determination of how the stellar rotation period varies as a function of age and mass (Rebull et al. 2016) and how the rate of flares from an active host star can affect the atmosphere of any orbiting exoplanet (Konings et al. 2022).

Determining the rotation period of low mass stars is usually based on the assumption that any modulation in the stars light curve is due to the rotation of a starspot(s) which come into and out of view as the star rotates. For stars whose rotation axis is viewed near face-on, it is expected that starspot(s) would remain

in view and show no modulation unless the spot coverage varied over time. Initially it was assumed that a single large spot group caused the modulation in a star's flux, with any variations in the rotation flux profile due to changes in the spot distribution or that additional starspots emerged. However, it has been shown that single filter photometry data can be reproduced by a wide range of spot distribution, sizes, inclinations and spot temperatures (Jackson & Jeffries 2013; Luger et al. 2021a). On the other hand, Luger et al. (2021b) argue that some degeneracies in the spot distributions can be broken by analysing the light curve of many stars which have broadly similar properties.

Although there is still some uncertainty in mapping the distribution of spots over the surface of these stars, progress has been made in searching for activity cycles on stars other than the Sun. The Solar cycle lasts  $\sim 11$  yr (strictly speaking  $\sim 22$  yr) and manifests itself through the changing number of sunspots; emission in the core of the Ca II H&K lines; X-ray flux and the number of flares and Coronal Mass Ejections. Given the timescales expected (years), finding evidence for stellar activity cycles took time to emerge. Systematic and regular spectroscopic observations of Solar-like stars began during the 1960's with a focus on using the Ca II H&K lines as an activity indicator (Wilson 1968). Subsequent studies using data such as these showed that other stars exhibit activity cycles on a similar timescale to the Sun (e.g. Baliunas et al. (1995) and references therein). For lower mass stars, an activity cycle of  $\sim 7$  yr was detected in the star nearest to the Sun, Proxima Centauri (M5.5Ve), using optical, UV and X-ray observations (Wargelin et al. 2017). Furthermore, Ibañez Bustos et al. (2020) used Ca II H&K lines to determine a stellar cycle of  $\sim 4$  yr in the M4V Gl 729. Kuker et al (2019) reviewed observations which appear to show that fast rotating M dwarfs have cycles of a year but increase to around four years

for slower rotators. However, fast rotators cannot be understood by an advection-dominated dynamo model.

In principle, ground based optical photometric observations which are stable and free from systematic trends can be used to detect activity cycles as long as the timeline is sufficiently long. Since 2018 the *TESS* satellite has gradually been building up a set of observations of stars covering most of the sky. This is particularly true for stars within  $\sim 11^\circ$  of the north and south ecliptic poles (the ‘continuous viewing zones’) since they can be observed for nearly one year with a return visit one year later. However, since these light curves are not flux calibrated, low amplitude, long term modulations or trends can be difficult to detect in a robust manner.

An alternative means is to search for variations in the amplitude of the rotational modulation over time (Berdyugina & Järvinen 2005). Using this approach, Suárez Mascareño et al. (2016) determined that two K type stars showed periods of 10.2 and 8.7 yr. Reinhold et al. (2017) used *Kepler* data to study the light curves of 23601 stars and used the Generalised Lomb Scargle Periodogram (LSP) to search for variations in the rotational amplitude with time and found amplitude periodicities in 3203 stars, with weak evidence that the cycle period increased for longer rotation periods. Most of the stars in that sample had spectral types earlier than MV stars. For a recent review of activity cycles on stars other than Sun see Jeffers et al. (2023).

In this exploratory study we use *TESS* data of low mass stars located in the north and south continuous viewing zones on two occasions to assess how stable the dominant period in their light curves is. For stars which showed very stable periods we searched for amplitude variations which may reveal evidence of stellar activity cycles.

## 2. The TESS sample

The *TESS* satellite was launched into an Earth orbit with a period of 13.7 d. It has four 10.5 cm telescopes that observe a  $24^\circ \times 90^\circ$  instantaneous strip of sky (a sector) for  $\sim 27$  d (see Ricker et al. 2015, for details). In the first year (Cycle 1) *TESS* covered most of the southern ecliptic hemisphere and in the second year (Cycle 2) it covered the northern ecliptic hemisphere, although with less sky coverage than Cycle 1 to avoid contamination from stray Earth and Moon-light. In both Cycles, there is an area around the ecliptic poles which are visible in each sector. In Cycle 3 the field pointings mirrored Cycle 1 and in Cycle 4, some sectors observed in Cycle 2 were observed again in addition to some fields not previously observed. In Cycles 1 and 2, full frame images were obtained every 30 min, which increased to every 10 min in Cycles 3 and 4. From the start, the Guest Observer programme was able to populate targets which were observed in a 2-min cadence, with a 20 s cadence option becoming available in Cycles 3 and 4.

We used the *Gaia* EDR3 catalogue of stars within 100 pc (Smart et al. 2021) and using their  $(BP - RP)$  colour and  $M_G$  absolute magnitude we selected those which had an equivalent spectral type later than  $\sim M0V$  and were on, or close to, the main sequence. We then cross matched this sample with those stars which had *TESS* light curves derived using the *TESS* Science Processing Operations Center FFI Target List Products (SPOC, Caldwell et al. (2020)) which uses the full-frame images to extract light curves (we searched light curves from *TESS* sectors 0–61). Since our aim was to search for variations in the amplitude of the main period, we then restricted our sample to require a star to have been observed in at least 6 sectors. Finally, since the pixel size of *TESS* ( $21''$  per pixel) is sufficiently large to include

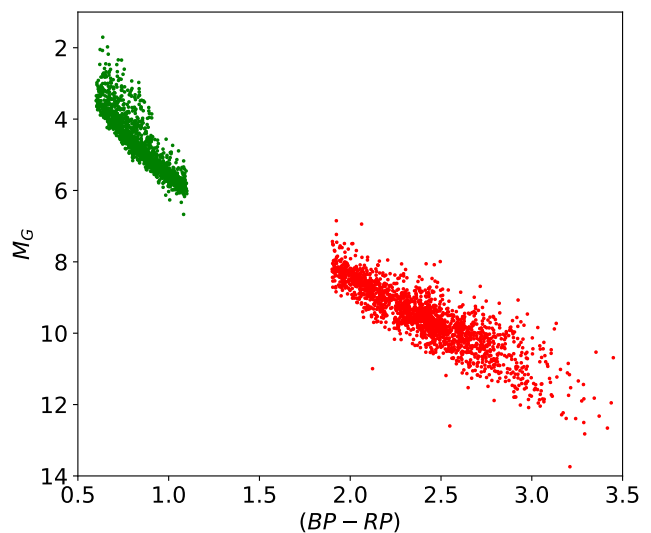


Fig. 1: The *Gaia* HRD ( $BP - RP$ ,  $M_G$ ) of low mass stars (red) and Solar type stars (green) which were observed for at least six sectors in each *TESS* Cycle.

spatially nearby bright stars to contaminate the resulting light curve, we filtered stars so the Contamination Ratio (Stassun et al. 2018) (i.e. the fraction of the flux from other spatially nearby stars) is  $< 0.1$ . We show in Figure 1 the 1950 stars which are our M dwarf sample. For a comparison, we also obtained a Solar-like sample using the same criteria as for M dwarfs, where we took stars close to the main sequence for  $0.6 < (BP - RP) < 1.1$  (F5V–K2V, Pecaú & Mamajek (2013)): we identified 1432 stars and these are shown as green dots in Figure 1.

## 3. Data analysis

Each sector of data was normalised so its mean was unity and then clipped to remove data which was  $5\sigma$  deviation from the mean. For each sector of data we used the LSP, as implemented in the VARTOOLS suite of tools (Hartmann & Bakos 2016; Zechmeister & Kürster 2009), to search for evidence for periodic variability. For each star we determined the period of the highest peak in the LS power spectrum in each sector of data in the range 0.08–10 d; its False Alarm Probability (FAP) and the full amplitude (which we shorten to amplitude for the rest of the paper) of the modulation for each sector was determined. We then obtained the median value for these parameters for each star. Since the lightcurves can still have systematic trends present even after a global trend has been removed, this can cause peaks in the LSP which are not astrophysical. In addition, the observing window can cause peaks in the LSP, even at periods which are a higher harmonic of the window length. Setting a threshold for the FAP to determine if a star shows significant variability is therefore not always clear cut (e.g. Anthony et al. (2022)) and red-noise can result in peaks in the LSP which technically have a  $FAP < 0.01$  (e.g. Dorn-Wallenstein et al. (2019)).

We therefore use the approach of Lu et al. (2022), who determined the spread in the period in different quarters of *Kepler* data using:

$$\Delta_{LS} = \frac{1}{N_S \langle P_{LS,s} \rangle} \sum_s |P_{LS,s} - \langle P_{LS,s} \rangle|, \quad (1)$$

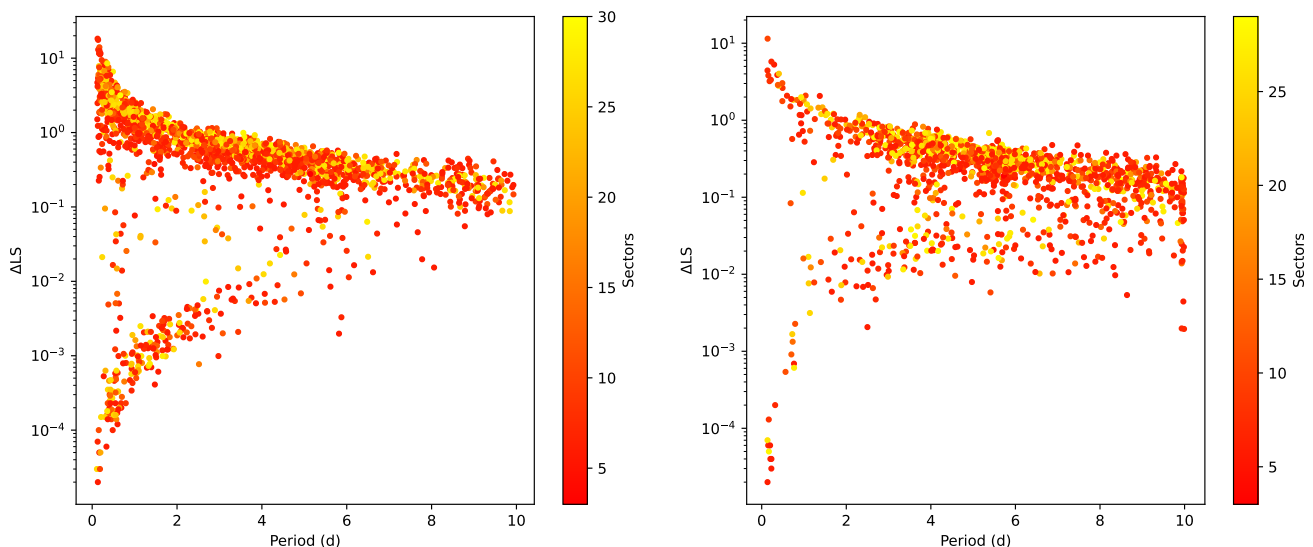


Fig. 2: Left hand panel: For all the 1950 M dwarf stars in the sample we determined the median period from their individual light curves and calculated  $\Delta_{LS}$ . Higher values of  $\Delta_{LS}$  indicate a greater spread in the values of the period over the sectors in which they were determined. The colours of the points indicate how many sectors of data were analysed. Right hand panel: The same distribution but for the 1432 stars in our Solar-like sample.

where  $N_S$  is the number of sectors with measured  $P_{LS,s}$ , and  $\langle \dots \rangle$  denotes the median value operator. We do not necessarily expect the rotation period of active stars to be *strictly* periodic, and therefore have very low values of  $\Delta_{LS}$ , since active regions can emerge and vanish at different latitudes over the sequence of the observations, which together with differential rotation of the star can lead to slightly different observed periods.

Since the LSP can identify half the real period when pulse profiles are double peaked, we determined the median period and  $\Delta_{LS}$  and then recomputed  $\Delta_{LS}$  so that if an individual sector was half the median period (within a few percent) we used twice this value and redetermined  $\Delta_{LS}$ . We show the median period and its spread ( $\Delta_{LS}$ ) for all 1950 stars in the left hand panel of Figure 2. There are two clear groupings: a band of points starting at the lower left which have very low  $\Delta_{LS}$  values which progress to higher values as the period increases. A second group of points starts in the top left hand corner which have a large spread in  $\Delta_{LS}$  which decreases as the period increases.

We examined the light curves and periodograms for stars which had median periods shorter than 2 d but had values of  $\Delta_{LS}$  higher than the strip of sources with low  $\Delta_{LS}$ : we found evidence for some stars appearing to be pulsators and others which had a longer period modulation super-imposed on the shorter period seen in an earlier Cycle of observations. This suggests that at least some stars above the band of stars seen in the low  $\Delta_{LS}$  strip are probably real variable stars but not isolated single M dwarfs which have starspots. Of course many others are likely not real variable stars and the LSP has just picked random peaks in the power spectrum which are likely due to red noise.

We now make a comparison with the Solar-like sample discussed in Sect. 2. We applied exactly the same procedures as we did for the M dwarf sample. Given Solar-type stars are expected to show (in general) rotation periods much longer than a few days (e.g. McQuillan et al. (2014)) we would not expect to see the same band of points at the lower left – unless their periods were spurious. We show the distribution of the 1432 Solar-type stars in the right hand panel of Figure 2: we find the same spread of points with high  $\Delta_{LS}$ , but only a few stars in the lower left. There are 17 Solar-like stars which appear to show very stable

periods (Figure 2). We searched the SIMBAD<sup>1</sup> database for information on these stars and found they were a mixture of eclipsing binaries; eruptive variables and Red Clump low mass core He burning stars (e.g. Ruiz-Dern et al. (2018)). We conclude they are not single star solar-like pulsators but other types of variable star, which gives support to the view that the majority of stable periodic low mass stars (left hand panel of Figure 2) are single low mass stars which have long lived starspots.

In selecting those sources with which to search for changes in the amplitude of variability we observe that in both samples, there is a ‘natural’ split between most sources which have  $\Delta_{LS} > 0.05$  and  $\Delta_{LS} < 0.05$ . We therefore identified 245/1950 M dwarfs and 194/1432 solar-type stars which have  $\Delta_{LS} < 0.05$  for the next stage of our analysis.

#### 4. Searching for variations in the rotational amplitude

Since the number of amplitude measurements per star is small (a maximum of 30 spread over five years) we need to identify a suitable statistical test which can robustly identify variations or trends in the data. In order to achieve this, we have used two different non-parametric tests for variability in the time series i.e. the Mann-Kendall (*MK*) test for monotonic trends in time series (Mann 1945; Kendall 1975) and a modified (non-parametric) version of the *R*-statistic introduced in Baptista & Steiner (1993). The *MK* test is sensitive to monotonic (both linear and non-linear) trends in the data, whilst the  $R_{np}$ -test measures the temporal distribution of the signs of the residuals  $r_i$  after subtracting the mean level from the time series. We define  $R_{np}$  as:

$$R_{np} = \frac{1}{\sqrt{N-1}} \sum_{i=1}^{N-1} \frac{r_i r_{i+1}}{|r_i| |r_{i+1}|} \quad (2)$$

where  $r_i$  are the time series residuals after subtracting the mean level.  $R_{np}$  follows a discrete normal distribution with a mean 0.0

<sup>1</sup> <https://simbad.cds.unistra.fr/simbad/>

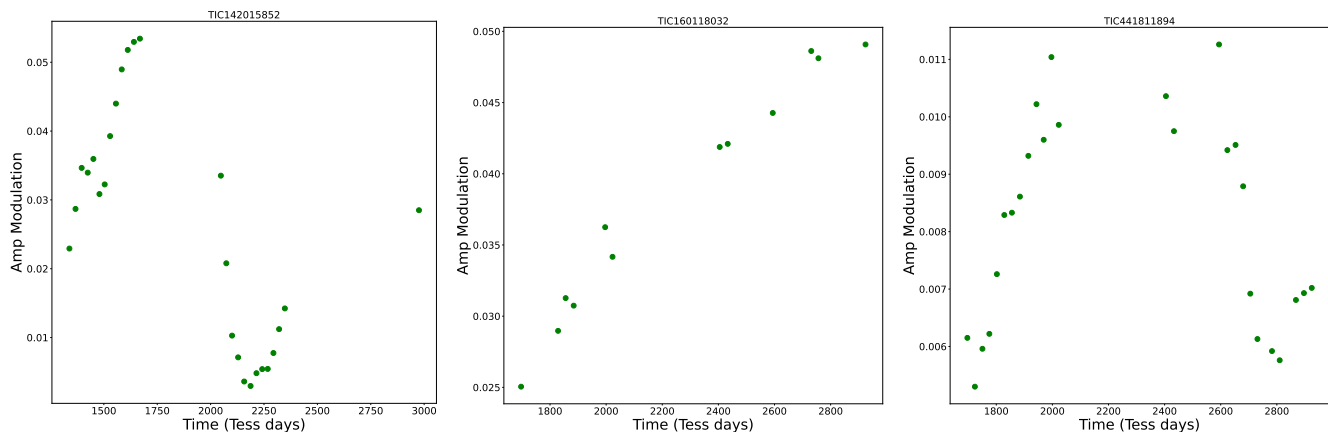


Fig. 3: Three examples of low mass stars, TIC 142015852, TIC 160118032, TIC 441811894, which have a variable rotational amplitude.

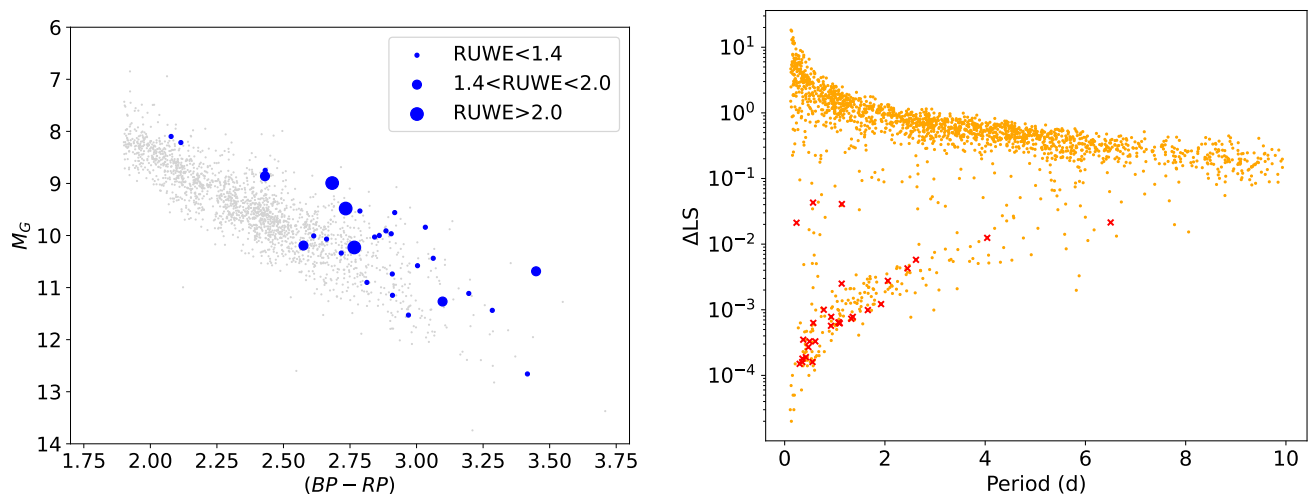


Fig. 4: Left hand panel: The *Gaia* HRD ( $BP - RP$ ,  $M_G$ ) of low mass stars (grey) with those identified as showing significant variability of the rotational amplitude over time shown as circles whose size indicates their *Gaia* RUWE value (see text for details). Right hand panel: The low mass star sample (orange dots) with the 29 stars which were identified as having a rotational amplitude which varies significantly over time shown as a red  $\times$  symbol.

and  $\sigma = 1.0$ . Large positive values of  $R_{np}$  correspond to cases where a number of consecutive datapoints show the same sign (either + or -) in their residuals after subtraction of the mean, i.e. the constant value model does not fit the data. The large negative values of  $R_{np}$  would imply systematically alternating consecutive residuals with opposite signs and could only arise if the data contained a short period that roughly matches the sampling period. This case is not relevant here. The probability distribution for  $R_{np}$  is discrete Gaussian, even if the data distribution would not be known. This enables us to obtain reliable probabilities for  $R_{np}$  values, even in the case of a small number of points.

These two tests are sensitive to different types of variability (monotonic trend vs. correlated/systematic residuals for a constant model), that can be present in the data. We therefore selected those stars whose amplitude variation over time gave a  $FAP < 0.0001$  with either the *MK* stat or the  $R_{np}$ -stat and had a minimum of 6 data points: this resulted in 29 low mass stars (if we choose  $FAP < 0.001$  we obtain 53 stars). The details of these 29 stars are shown in Table 1 with three example light curves showing the amplitude variation over time is shown in Figure 3 (the amplitude variation of all 29 stars are shown in Figure A.1–A.3). There is a range of light curve characteristics such as TIC

142015852 which shows a rise to maximum followed by a dip 1.5 yrs later; TIC 160118032 which shows a continuous increase amplitude over 3 yrs and TIC 441811894 which shows a rise followed by a decline several years later. In contrast, we found evidence for only one star in our solar-like sample (TIC 38707949) which showed a general decrease in rotational amplitude over a timescale of 2.5 yrs.

We also show the 29 stars in the *Gaia* HRD in the left hand panel of Figure 4 which shows that they are biased towards the red or more luminous parts of the lower main sequence. This may imply the stars are younger compared to the overall sample or they are members of binaries. To explore this further, we indicate using the colour of the points the *Gaia* Renormalised Unit Weight Error (RUWE) parameter for each of the 29 stars. This is a measure of how much the photo-center of a star moves over the course of the *Gaia* observations (Lindegren et al. 2021a). Initial indications suggest that for stars with  $RUWE > 1.4$  the star is an unresolved binary system (Lindegren et al. 2021b), although this does not preclude that binaries can have  $RUWE < 1.4$  (Stassun & Torres 2021) and that the distribution of RUWE can vary over the *Gaia* HRD (Penoyre et al. 2022). We cross matched our 29 low mass stars with the resulting catalogue of binaries within

100 pc from (Penoyre et al. 2022) finding that only two sources with the highest RUWE ( $>5.5$ ) were in their catalogue. However, 7 out of these 29 stars have  $RUWE > 1.4$  suggesting they are possibly binary systems.

We folded and phase binned the data on the period identified for that sector and show six examples in Figure 5. Two of the stars were in the binary sample derived by Penoyre et al. (2022). Another one star, TIC 38586438, is an eclipsing binary. We show the folded light curves for three stars which are representative of the other stars in the sample.

In the right hand panel of Figure 4 we show a similar plot as the left hand panel of Figure 2 but highlighting the location of the 29 low mass stars which we identified as having variable amplitudes. Out of the 29 stars, 26 are located in the band of stars with low  $\Delta_{LS}$  values. All the stars have periods shorter than 7 days. There are three stars which have periods shorter than 2 days and have  $\Delta_{LS}$  values much higher than the others. One of these (TIC 33881250) has one sector where the period of the highest peak differs from the others and has a much higher FAP, although several flares could have interfered with the period determination. Another two stars (TIC 149347629 and 441811894) show two periods with the highest peak changing: this may indicate they are pulsators. We therefore do not consider these stars in the next stage of the analysis and are left with 26 stars.

## 5. Expected length of stellar cycles in low mass stars

Using measurements of the Ca II H&K lines using data taken at Mt Wilson from the 1960's (Wilson 1968), Brandenburg et al. (1998) found evidence that the ratio of the period of the activity cycle,  $P_{cyc}$ , and the stellar rotation period,  $P_{rot}$ , was related to the Rossby number ( $R_o = P_{rot}/\tau$ ), where  $\tau$  is the convective turnover time. More recently, Irving et al. (2023) searched for a relationship between  $P_{cyc}/P_{rot}$  and  $R_o$  for Solar-like and M dwarf stars. For the latter they determined  $P_{cyc}/P_{rot} = 3.6 R_o^{-1.02}$  (see Fig 16 and eqn 4 of Irving et al. (2023)). Based on this relationship we calculated what the predicted  $P_{cyc}$  for the stars in our sample would be. We assume that the period we measure from the *TESS* data is the stars rotation period.

Because  $R_o$  is not an observable quantity, we have to use a proxy. One established means is that derived by Wright et al. (2018) who use the  $(V - K_s)$  colour to derive  $\tau$ . However, Irving et al. (2023) using work of Corsaro et al. (2021), Landin et al. (2023) and Pecaute & Mamajek (2013), derived new relationships for  $(V - K_s)$  and  $\tau$ . For  $(V - K_s) < 4.6$  (stars earlier than M3V) the resulting values of  $\tau$  are similar to that of Wright et al. (2018). Following Irving et al. (2023) we use the  $\tau_L$  relationship for  $(V - K_s) < 4.6$  and  $\tau_G$  for  $(V - K_s) > 4.6$  (see Figure 13 of Irving et al. (2023): for those stars near the boundary we chose the higher value). The values of  $\tau$  for each star are shown in Table 1. Using  $\tau$  and the period for each star we compute  $R_o$  and use the relationship of Irving et al. between  $P_{cyc}/P_{rot}$  and  $R_o$  to determine the length of the activity cycle of our stars. We show the predicted cycle lengths in Table 1 which range from 0.6–4.6 yrs: they are longer by a factor of  $\sim 2-7$  compared to the values determined by simply using the relationship of Wright et al. (2018).

The amplitude variation over time is shown for all stars in Figures A.1 and A.3. In order to estimate the length of the activity cycles from the amplitude time series data, we experimented with fitting the amplitude time series with a Fourier series models with different number of harmonic terms and also the period

as a free parameter. Such a problem is non-linear and thus we carried out extensive MCMC fitting to derive limits/probability distribution for any activity periods. However, we were not able to obtain repeatable and reliable results. This is due to the gaps in the time series, and the length of the trends. However, it is clear that some stars such as TIC 441734910 have a downward trend lasting  $\sim 3.5$  yrs implying any activity cycles could be  $\sim 8-10$  yrs. The predicted activity cycle based on the relationship of Irving et al. (2023) is 7.2 yrs. In contrast, TIC 142015852 shows an amplitude variation which is consistent with a timescale of  $\sim 3$  yrs: the predicted cycle length is 1.3 yrs. This gives us modest confidence that the variations which we observe are of the same order as the predicted timescales for activity cycles.

## 6. Amplitude variation as a function of rotation period

We determined the range in the amplitude over time by simply taking the difference between the maximum and minimum values for each of the 26 stars. The fractional mean amplitude ‘Max-Min’ is 0.022, with a range between 0.005 and 0.063. We then searched for a correlation between Max-Min and the stars mass, temperature (from the TIC, Stassun & Torres (2021)) and rotation period. We used the Kendall  $\tau$  test to determine the significance of any correlation. We found no evidence for a correlation between mass or temperature. However, we found a FAP for the rank correlation between the amplitude variation and modulation period of 0.00587 (Figure 6). (A similar result was found when we compare the amplitude variation with Rossby number). Although this implies a 99.41 percent probability that the correlation is real, it does not formally reach the  $3\sigma$  level. The one outlying point is TIC 341870349 ( $P_{rot} \sim 4$  d), although it is not obvious why this is the case.

Although statistical confidence in the correlation does not formally reach the  $3\sigma$  level, we note that stars showing a larger range in the amplitude of modulation are likely to have a greater asymmetry in the distribution of spots than stars showing a smaller modulation. It may imply stars which are faster rotating (and therefore likely young) have spots more uniformly distributed and covering a larger fraction of their photosphere.

## 7. Discussion

There is now robust evidence from spectroscopic observations that Solar-like stars can show stellar activity cycles similar in duration to that found in the Sun. This is because of the length of observations, such as initiated at Mt Wilson (Wilson 1968), but also more recent high precision spectroscopy from instruments such as HARPS (Lovis et al 2011). Obtaining similarly robust claims for other stars such as M dwarfs using photometric measurements is difficult since all-sky precise photometry is still challenging (e.g. Stubbs & Tonry (2006)). We also note that most claims of significant detections of periods in photometric data are made using the LSP which assume that data have a Gaussian noise profile whereas almost all such data streams contain red noise which result in FAP's which are far lower than they are in reality (e.g. Littlefair et al. (2017)). Similarly, Basri & Shah (2020), using simulations of starspot distributions, show that ‘short’ activity cycles (of the order of several tens or more rotation cycles) are simply due to random processes.

In this exploratory study, we have gone to great lengths to identify stars which have very stable photometric periods over a timescale of several years. As a result we have found 26 low

Table 1: Details of the 29 low mass stars which show a significant variability in their rotational amplitude over time.

TIC	RAJ2000	DEJ2000	Gmag	imag	MG	BP-RP	MedPer (d)	RUWE	$(V - K_s)$	$\tau$ (d)	$P_{\text{predict.cyc}}$ (yr)
33881250	66.342433	-76.501968	14.23	13.35	10.4	3.06	1.141	1.33	5.72	360	3.1
38515801	62.551500	-63.856128	14.57	13.68	10.0	2.86	1.072	1.19	5.50	370	3.7
38586438	64.090211	-62.012890	12.83	12.03	8.9	2.43	0.556	1.53	4.65	420	6.9
142015852	96.591637	-75.277925	12.45		8.1	2.08	2.622	1.24	4.05	60	1.3
142082942	98.259771	-72.762015	14.23	13.34	10.9	2.81	0.924	1.10	5.42	370	3.8
149347629	83.648302	-60.182846	14.13	13.25	9.8	3.03	0.566	1.10	5.68	360	3.2
160118032	231.210928	83.991618	14.61	13.93	10.1	2.66	0.351	1.16	5.03	400	5.2
176980970	101.601200	-70.634179	14.57	13.72	10.0	2.84	0.611	1.18	5.34	380	4.1
177313167	103.849793	-74.048574	14.21	13.33	11.5	2.97	0.300	1.20	5.53	370	3.6
198557860	238.295269	62.595799	14.50	13.79	11.1	3.20	0.423	1.28	5.69	360	3.2
219773818	263.311581	63.207745	14.56	13.86	12.7	3.42	1.138	1.11	6.26	350	2.2
230384382	285.730684	60.586065	14.72	14.04	10.2	2.77	0.497	5.56*	4.93	400	5.5
230395228	286.673233	63.754117	13.69	12.82	10.6	3.00	0.780	1.17	5.23	380	4.4
233547261	281.738333	60.895959	14.46	13.77	10.0	2.61	2.451	1.14	4.98	400	5.4
271693722	109.549273	-75.347401	14.71	13.86	10.3	2.72	1.923	1.19	4.97	400	5.4
278825715	100.316544	-56.275061	13.46	12.56	9.5	2.79	6.503	1.24			
294329266	109.049841	-58.814441	13.50	12.64	9.5	2.73	0.370	2.44	5.32	380	4.2
300866996	117.229923	-67.359987	14.32	13.37	10.7	3.45	0.355	1.84	6.64	350	1.8
306779230	121.428627	-71.190802	14.41	13.52	9.6	2.92	1.329	1.16	5.73	350	3.0
339770560	111.121245	-59.372994	13.86	12.99	9.9	2.89	1.098	1.15			
341870349	276.732905	71.413962	13.22	12.61	8.7	2.43	4.041	1.27	4.61	420	7.0
349192028	108.836918	-60.377753	12.86	12.14	8.2	2.11	2.059	1.30	4.08	60	1.3
350559457	86.563846	-55.797830	14.66	13.74	11.4	3.28	0.571	1.05	6.16	350	2.4
353898013	271.899854	56.324229	13.94	13.35	10.7	2.91	1.659	1.19	5.29	380	4.3
375035131	99.647221	-62.560617	14.77	13.85	10.0	2.90	0.928	1.09	5.56	370	3.5
382147080	80.523154	-55.826228	13.52	12.65	9.0	2.68	0.473	6.24*	4.95	400	5.5
402897917	302.768145	68.500219	14.69	13.99	11.1	2.91	1.088	1.03	5.33	380	4.2
441734910	258.253191	73.934726	12.72	12.13	10.2	2.58	1.359	1.43	4.57	420	7.2
441811894	266.958528	73.176166	14.34	13.40	11.3	3.10	0.236	1.72	5.42	380	4.0

**Notes.** An asterisk in the RUWE column implies it has been classed as a binary in Penoyre et al. (2022), while the folded light curve of TIC 38586438 shows it is an eclipsing binary (Figure 5). We also show the  $(V - K_s)$  value from the TIC, the convective turnover time,  $\tau$ , and the predicted length of the activity cycle both derived from the relationships in Irving et al. (2023). Stars TIC 33881250, 149347629 and 441811894 are the stars with periods  $< 2$  d showing higher values of  $\Delta_{LS}$  than the other stars with crosses in the right hand panel of Figure 4.

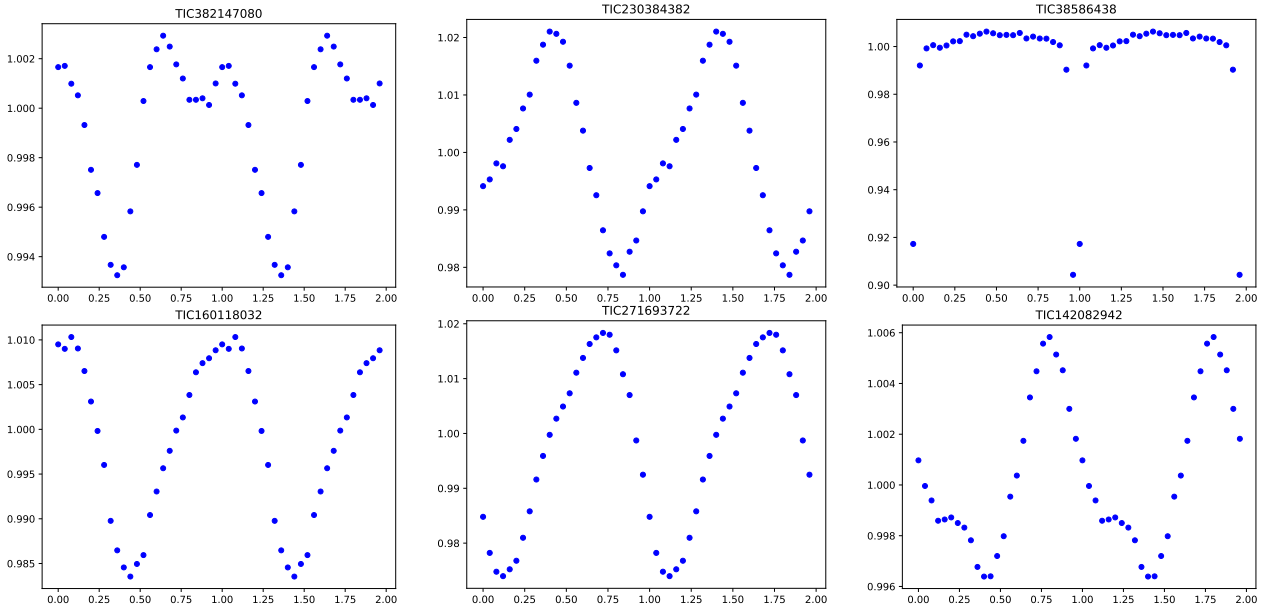


Fig. 5: The first sector of data for six stars in our M dwarf sample which have been folded and binned on the period of the highest peak in the LSP – the phase is arbitrary. The left hand and middle stars in the upper panel are in the binary sample of Penoyre et al. (2022) while TIC 38586438 appears to be an eclipsing binary. The shape of the folded light curves of TIC 160118032, 271693722 and 142082942 are representative of other stars in the sample.

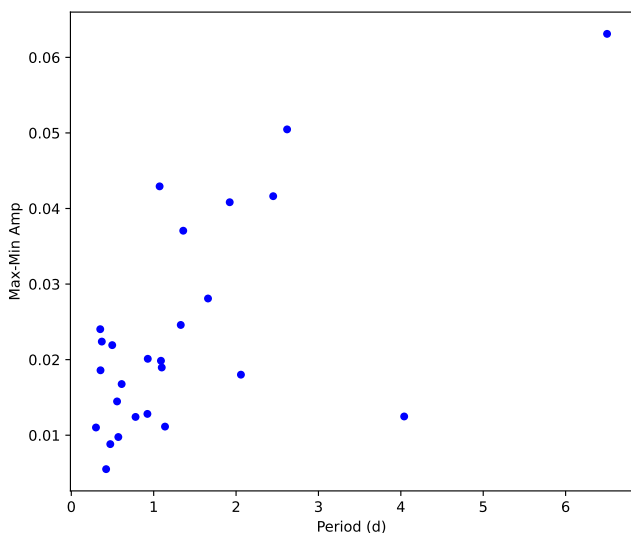


Fig. 6: The variation in the amplitude of the modulation over the course of their observation as a function of modulation period. There is a marginally significant trend in the size of the amplitude variation over period.

mass M dwarfs which show evidence for a significant variation in the amplitude of their rotational modulation over a time interval of nearly five years. There are some stars whose amplitude variation points to a long term cycle of up to ten years and there are other stars whose timescale is  $\sim 3$ –4 yrs. Given the relatively short rotation periods, we do not consider these to be equivalent of spurious activity cycles noted by Basri & Shah (2020).

Compared to Solar-like stars, the number of low mass stars (MV and later) which have robustly determined activity cycles from spectra is much fewer, partly because they are fainter in the blue where the activity marker Ca II H&K lines are present. Suárez Mascareño et al. (2016) used photometric data obtained using the All Sky Automated Survey (ASAS) to search for activity cycles and found 25 early M and 9 mid M spectral types – these samples were biased towards relatively long rotational periods, a median of 33.4 d (early M) and 86.2 d (mid M). In the sample of Irving et al. (2023) which was mentioned in Sect. 5, of their 15 stars, four had periods shorter than 6 d and only one with a period shorter than 2 d. Our sample of 26 stars therefore reveals a set of low mass stars which are rapidly rotating and have potential activity cycles.

## 8. Conclusion

In this pilot study, we examined the *TESS* light curves of 1950 low mass and 1432 Solar-type stars. We found that only 245 (12.6%) low mass stars showed stable periods over many sectors compared to 194 (13.5%) Solar-type stars – we assume that these periods are a signature of the stars rotation period. However, there are many more low mass stars which show very stable periods at periods shorter than  $\sim 4$  d than Solar-type stars. This implies that the low spread in measured periods of the short period M dwarfs is real and not produced by sampling or any artefacts in the data. We note that the FAP of periods detected using the LSP can give periods which may appear to be significant at the 1% level (which is commonly used in the literature) which are in fact due to red noise.

We searched for variations in the amplitude of the rotation period using two statistical tests and find that 29 low mass stars

and one Solar-type star shows evidence for significant variability. The *TESS* light curves of stars in the continuous viewing zones all have gaps of one year. This makes determining any meaningful estimate of the period of variation difficult. However, they are not widely inconsistent with the predicted cycle length which is based on the stars Rossby number.

One mission which will observe the same field continuously is ESA’s *PLATO* mission which is due to be launched in Dec 2026 and will make an initial pointing in the southern hemisphere lasting at least 2 yrs (Nascimbeni et al. 2022) covering a continuous area of  $1037 \text{ deg}^2$ . Since this field will have been observed a number of times using *TESS* it will provide the means to study the modulation amplitude of thousands of stars over a time interval comparable or longer to the expected activity cycles.

Another means to fill the gaps is ground based wide-field optical surveys such as *GOTO* (Steeeghs et al. 2022; Dyer et al. 2022), or *ATLAS* (Tonry et al. 2018), which have telescopes in both hemispheres are perfectly placed to fill in the gaps when *TESS* is not able to observe parts of the sky, if they make extended observations of the same fields every few months. It would also be interesting to determine if there is any variation in the X-ray flux of the 26 stars found to show long term variability in their rotational amplitude. We hope that eRosita (Predehl et al. 2021) can resume operations in the near future.

*Acknowledgements.* This paper includes data collected by the *TESS* mission, for which funding is provided by the NASA Explorer Program. This work also presents results from the European Space Agency (ESA) space mission *Gaia*. *Gaia* data is being processed by the *Gaia* Data Processing and Analysis Consortium (DPAC). Funding for the DPAC is provided by national institutions, in particular the institutions participating in the *Gaia* MultiLateral Agreement (MLA). The *Gaia* mission website is <https://www.cosmos.esa.int/gaia>. The *Gaia* archive website is <https://archives.esac.esa.int/gaia>. Armagh Observatory & Planetarium is core funded by the N. Ireland Executive through the Dept. for Communities. JGD would like to thank the Leverhulme Trust for a Emeritus Fellowship.

## References

- Anthony, F., et al. 2022, *AJ*, 163, 257  
 Baliunas, S. L., et al., 1995, *ApJ*, 438, 269  
 Baptista R., Steiner J. E., 1993, *A&A*, 277, 331  
 Basri, G., Shah, R., 2020, *ApJ*, 901, 14  
 Berdyugina, S. V., Järvinen, S. P., 2005, *Astron. Nachr*, 326, 283  
 Brandenburg, A., Saar, S. H., Turpin, C. R., 1998, *ApJ*, 498, L51  
 Caldwell, D. A., *RNAAS*, 4, 201  
 Corsaro, E., Bonanno, A., Mathur, S., et al. 2021, *A&A*, 652, L2  
 Davenport, J. R. A., 2016, *ApJ*, 829, 23  
 Dorn-Wallenstein, T. Z., Levesque, E. M., Davenport, J. R. A., 2019, *ApJ*, 878, 155  
 Doyle, J.G., Butler, C.J., Callanan, P.J., Tagliaferri, G., de La Reza, R., White, N.E., Torres, C.A., Quast, G., 1988a, *A&A* 191, 79  
 Doyle, J.G., Butler, C.J., Byrne, P.B., van den Oord, G.H.J., 1988b, *A&A* 193, 229  
 Doyle, J.G., Mathioudakis, M., Murphy, H.M., Avgoloupis, S., Mavridis, L.N., Seiradakis, J. H., 1993, *A&A* 278, 499  
 Dyer, M. J., et al., 2022, *SPIE*, 121821, 1Y  
 Hartman, J. D., Bakos, G. Á., 2016, *A&C*, 17, 1  
 Henry, T. J., Jao, W.-C., Subasavage, J. P., Beaulieu, T. D., Ianna, P. A., Costa, E., Méndez, R., A., 2006, *AJ*, 132, 2360  
 Ibañez Bustos, R. V., Buccino, A. P., Messina, S., Lanza, A. F., Irving, Z. A., Saar, S. H., Wargelin, B. J., do Nascimento, J.-D., 2023, *ApJ*, 949, 51  
 Jackson, R. J., Jeffries, R. D., 2013, *MNRAS*, 431, 1833  
 Jeffers, S. V., Kiefer, R., Metcalfe, T. S., 2023, *SSRv*, 219, 54

- Kendall, M.G., 1975. Rank Correlation Methods, 4th edition, Charles Griffin, London.
- Konings, T., Baeyens, R., Decin, L., 2022, A&A, 667, A15
- Küker, M., Rüdiger, G., Olah, K., Strassmeier, K. G., 2019, A&A, 622, A40
- Landin, N. R., Mendes, L. T. S., Vaz, L. P. R., & Alencar, S. H. P. 2023, MNRAS, 519, 5304
- Lindegren, L., 2021a, A&A, 649, A2
- Lindegren, L., 2021b, A&A, 649, A4
- Littlefair, S. P., Burningham, B., Helling, C., 2017, MNRAS, 466, 4250
- Lovis, C., et al. 2011, eprint arXiv:1107.5325
- Lu, Y., Benomar, O., Kamiaka, S., Suto, Y., 2022, ApJ, 941, 175
- Luger, R., Foreman-Mackey, D., Hedges, C., Hogg, D. W., 2021a, AJ, 162, 123
- Luger, R., Foreman-Mackey, D., Hedges, C., Hogg, D. W., 2021b, AJ, 162, 124
- Mann, H.B., 1945, Econometrica, 13, 163.
- McQuillan, A., Mazej, T., Aigrain, S., 2014, ApJS, 211, 24
- Nascimbeni, V. et al., 2022, A&A, 658, A31
- Pecaut M. J., Mamajek E. E., 2013, ApJS, 208, 9
- Penoyre, Z., Belokurov, V., Evans, N. W., 2022, MNRAS, 513, 5270
- Pettersen, B. R., 1989, SoPh, 121, 299
- Predehl, P., et al., 2021, A&A, 647, A1
- Rebull, L. M., et al., 2016, AJ, 152, 113
- Ricker G. et al., 2015, JATIS, 1a4003
- Reinhold, T., Cameron, R. H., Gizon, L., 2017, A&A, 602, A52
- Rodono, M., et al., 1986 A&A 165, 135
- Ruiz-Dern, L., Babusiaux, C., Arenou, F., Turon, C., Lallement, R., 2018, A&A, 609, A116
- Smart, R. L., et al., 2021, A&A, 649, A6
- Stassun, K., et al., 2018, AJ, 156, 102
- Stassun, K. G., Torres, G., 2021, ApJL, 907, 33
- Steehhs, D., et al., 2022, MNRAS, 511, 2405
- Stubbs, C. W., Tonry, J. L., 2006, ApJ, 646, 1436
- Suárez Mascareño, A., Rebolo, R., González Hernández, J. I., 2016, A&A, 595, A12
- Tonry, J. L., Denneau, L., Heinze, A. N., Stalder, B., Smith, K. W., Smartt, S. J., Stubbs, C. W., Weiland, H. J., Rest, A., 2018, PASP, 130, 064505
- Wargelin, B. J., Saar, S. H., Pojmański, G., Drake, J. J., Kashyap, V. L., 2017, MNRAS, 464, 3281
- Wilson, O. C., 1968, ApJ, 153, 221
- Wright, N. J., Newton, E. R., Williams, P. K. G., Drake, J. R., Yadav, R. K., 2018, MNRAS, 479, 2351
- Zechmeister, M. & Kürster, M., 2009, A&A, 496, 577

## **Appendix A: Long term variability of amplitude**

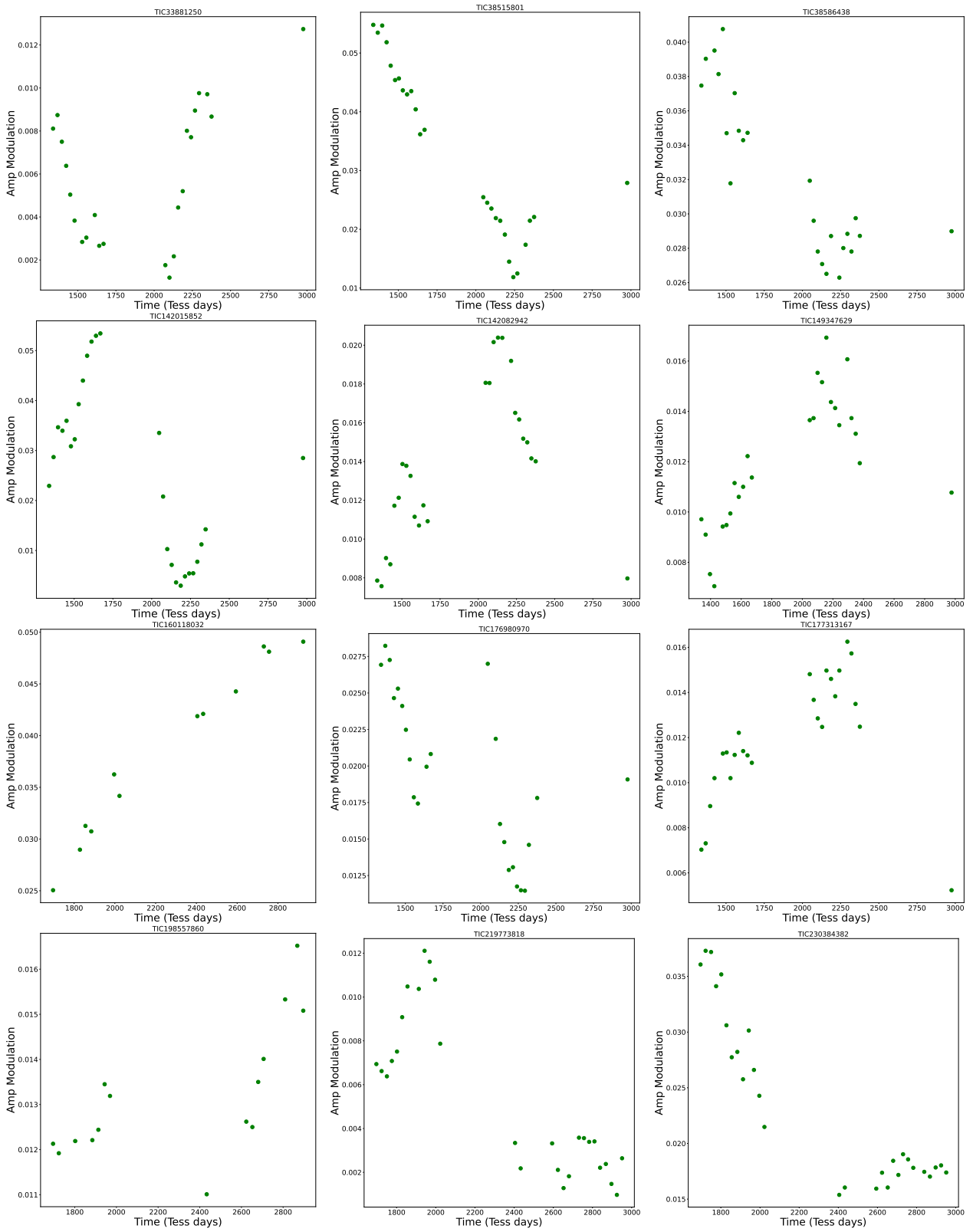


Fig. A.1: The amplitude of the rotational modulation of low mass stars which we have identified as showing significant variability.

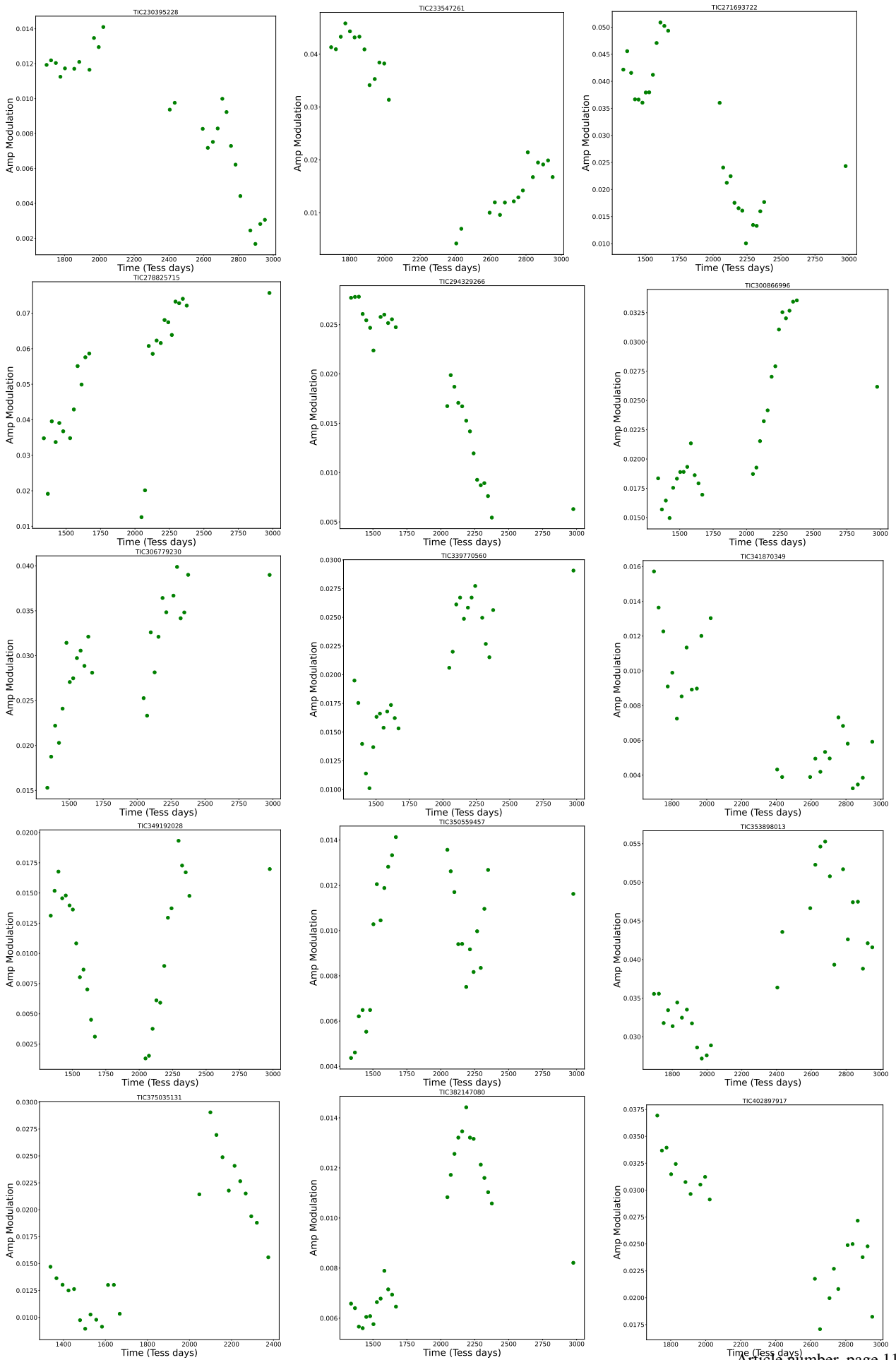


Fig. A.2: The amplitude of the rotational modulation of low mass stars which we have identified as showing significant variability (Cont).

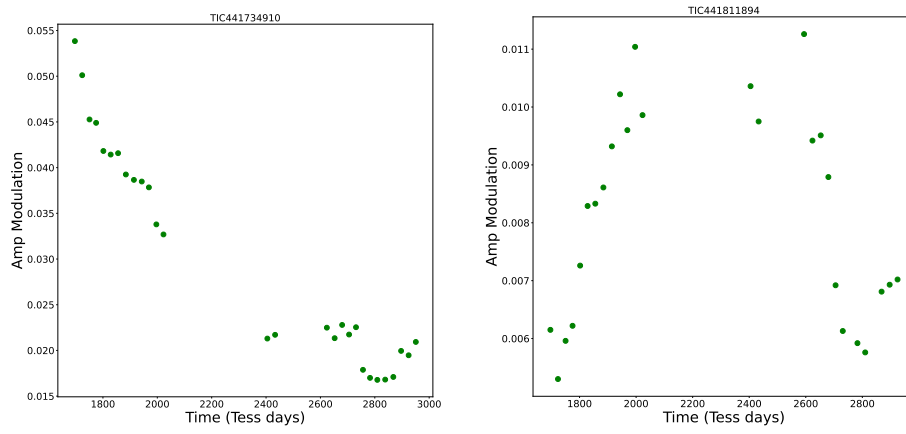


Fig. A.3: The amplitude of the rotational modulation of low mass stars which we have identified as showing significant variability (Cont).